Fluorescence induction of photosynthetic bacteria

G. SIPKA[*,**], M. KIS[*], J.L. SMART[***], and P. MARÓTI[*,+]

Department of Medical Physics, University of Szeged, Rerrich Béla tér 1, Szeged 6720, Hungary[*]
Department of Plant Biology, Hungarian Academy of Science, Biological Research Centre, Szeged, Hungary[**]
Department of Biological Sciences, University of Tennessee at Martin, USA[***]

Abstract

The kinetics of bacteriochlorophyll fluorescence in intact cells of the purple nonsulfur bacterium *Rhodobacter sphaeroides* were measured under continuous and pulsed actinic laser diode (808 nm wavelength and maximum 2 W light power) illumination on the micro- and millisecond timescale. The fluorescence induction curve was interpreted in terms of a combination of photochemical and triplet fluorescence quenchers and was demonstrated to be a reflection of redox changes and electron carrier dynamics. By adjustment of the conditions of single and multiple turnovers of the reaction center, we obtained 11 ms^{-1} and 120 μs^{-1} for the rate constants of cytochrome c_2^{3+} detachment and cyclic electron flow, respectively. The effects of cytochrome c_2 deletion and chemical treatments of the bacteria and the advantages of the fluorescence induction study on the operation of the electron transport chain *in vivo* were discussed.

Additional keywords: bacterial photosynthesis; electron transfer; fluorescence transients; intact cells.

Introduction

The science-based celebration of Govindjee's birthday should be inevitably connected to the Kautzky effect of characteristic kinetic changes of the chlorophyll (Chl) fluorescence of photosynthetic organisms upon light excitation (Kautsky and Hirsch 1931). First, he was born a year after the effect was discovered, and second, he has shown life-long commitment to the phenomenon of Chl fluorescence induction while fascinating and motivating two or three generations of plant scientists. Largely thanks to his pioneering and seminal works on the interpretation and evaluation of the Kautzky effect, there has been a long tradition to track the cyclic and noncyclic electron transfer in higher plants, cyanobacteria, and algae by kinetic changes of the Chl fluorescence (Stirbet and Govindjee 2012). However, considerably fewer investigations and much lower level of instrumentation have been devoted to the bacteriochlorophyll (BChl) fluorescence of photosynthetic bacteria. In an attempt to reduce this gap, and in honor of Govindjee, the subject of this work is devoted to the induction and relaxation of BChl fluorescence in the purple nonsulfur photosynthetic bacterium *Rhodobacter*

sphaeroides under various time and excitation ranges.

The topography of the photosynthetic apparatus of purple nonsulfur bacteria and the function of the macromolecular complexes including the intra- and interprotein electron transfer have been revealed with high precision (Niederman 2016). The system is set into operation by absorption of light in the light-harvesting complex. The electron excitation energy is funneled to the reaction center (RC) where an electron is stripped from BChl dimer (P) thereby acquiring a positive charge (P$^+$) (Fig. 1). The electron from the periplasmic site of the membrane is transferred *via* several different pigments to the acceptor quinone system ($Q_A Q_B$) on the cytosolic membrane face thus producing a charge separation P$^+$($Q_A Q_B$)$^-$ in the RC. After accepting two electrons from the same P, the quinone binds two protons from the cytosol, forming the reduced quinone QH_2, which is then released as a two-electron carrier from the RC. The flow of electrons from the lipid-soluble QH_2 to other acceptors proceeds *via* either a cyclic or noncyclic path. Following the cyclic pathway, the QH_2 diffuses to a cytochrome bc_1
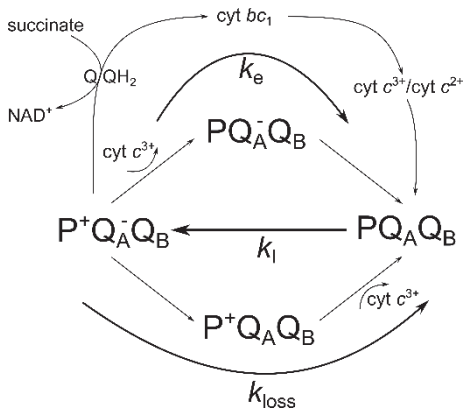
Fig. 1. A simplified scheme for stationary electron flows in and around the RC: light excitation closes the open RC (PQ_AQ_B) with rate constant k_I and the closed RC ($P^+Q_A^-$) is re-opened by electron transfer from the acceptor side, *via* the Q/QH_2 quinone pool in the membrane, the cytochrome bc_1 complex and the periplasmic cyt c, arriving at the donor side, P with overall rate constant k_e (cyclic electron transport). The noncyclic (reverse) electron flow from succinate to NAD^+ is connected to the cyclic flow at the Q/QH_2 quinone pool in the membrane. If any of the positive or negative charges cannot escape from the RC (predominantly at single turnover of the RC), the closed RC will be re-opened by a slow leakage of rate constant k_{loss}.

complex where it releases its two electrons to a site on the exoplasmic surface. Simultaneously, QH_2 releases two protons into the periplasmic space, thereby generating a proton-motive force which is used by the $F_0F_1ATPase$ to synthesize ATP and also to transport molecules across the membrane. Electrons are then transferred from the cytochrome bc_1 complex to a water-soluble cytochrome (cyt c_2), a one-electron carrier in the periplasmic space; this reduces the cytochrome from an Fe^{3+} to an Fe^{2+} state. The reduced cytochrome then diffuses through a small pool of cyt c_2^{3+}/cyt c_2^{2+} back to the RC, where it releases its electron to the positively charged dimer (P^+), returning it to the ground state P. In the case of the noncyclic pattern of reverse electron flow in purple nonsulfur bacteria, the electrons are removed from reduced organic molecules,

such as succinate and lactate, and are transferred to NAD^+ *via* the quinone pool in the membrane, forming NADH. In the noncyclic pathway, as in the cyclic pathway, a proton-motive force is generated and used to synthesize ATP.

In order to track the electron transfer steps and for the evaluation of the physiological status of the purple anoxygenic phototrophs, induction and relaxation of BChl fluorescence have largely prevailed (Koblizek *et al.* 2005, Maróti 2008, 2016; Asztalos *et al.* 2010, 2015; Kis *et al.* 2014, 2015). While the RCs are photooxidized and effectively become closed during the fluorescence induction phase, they open again during the fluorescence relaxation phase. The classic relation between the fluorescence yield and the fraction of closed RC has served as the basis for interpretation of fluorescence induction (Duysens 1951). When the RC is open (PQ_A), the fluorescence level is low (F_0) as part of the excitation energy is used for photochemistry (charge separation). However, when the RC is closed ($P^+Q_A^-$), the level of fluorescence is high (F_{max}) because photochemical loss no longer comprises the nonradiative dissipative pathway of the excited BChl. The difference between the maximum and minimum fluorescence (variable fluorescence $F_v = F_{max} - F_0$) reflects the redox status of the RC, and provides an estimate of the quantum yield of the primary charge separation (Trissl 1996, de Rivoyre *et al.* 2010).

In the present study, the fluorescence induction of the RC from *R. sphaeroides* is evaluated under high light (continuous) and moderate (intermittent) light intensities. The observed kinetic phases are the result of different types of fluorescence quenchers including photochemical quenchers (the oxidized quinones and the reduced dimer in the RC) and triplets of the excited states of BChl and carotenoids, and the ground state of oxygen. Under sufficiently low-light conditions, where the light-driven processes (charge separation and triplet formation) compete with electron transfer, a simple method is described to determine the overall steady-state rate of cyclic electron transfer in intact cells of *R. sphaeroides*. The effects of different electron transfer inhibitors and treatments of the bacteria are also discussed.

Materials and methods

Bacterial strains, culture conditions and chemicals: Purple nonsulfur photosynthetic bacterium *R. sphaeroides* wild type (WT) was grown in Sisström's medium (Sisström 1962) in completely filled screw top vessels without oxygen (anaerobic growth) under irradiance of 13 W m^{-2} from tungsten lamps (Asztalos *et al.* 2010). The cells were harvested at an exponential phase of the growth at cell concentration of $\sim 10^8$ cell mL^{-1} and were bubbled with nitrogen for 15 min before measurements to preserve the anoxic conditions.

Strain JS2293Δ, containing an in-frame deletion of the *cycA* gene encoding cytochrome c_2 in *R. sphaeroides*, was genetically constructed essentially as described previously

(Chi *et al.* 2015). *Escherichia coli* strains were grown at 37°C in LB medium (Sambrook *et al.* 1989) supplemented with antibiotics when appropriate; kanamycin (50 μg mL^{-1}) and ampicillin (100 μg mL^{-1}). *R. sphaeroides* strains were grown aerobically at 30°C in YCC medium (Sisström 1977) supplemented when appropriate with kanamycin (50 μg mL^{-1}). Conjugal transfer of strains from *E. coli* to *R. sphaeroides* was performed as described previously, and counter-selection against S17-1 donors was achieved by addition of tellurite (100 μg mL^{-1}) (Donohue and Kaplan 1991).

Terbutryne was used in 120 μM concentration to block the $Q_A \rightarrow Q_B$ interquinone electron transfer in the RC as

terbutryne competes with quinone for the Q_B-binding site. Myxothiazol was used in 10 μM concentration to inhibit the cyclic electron transfer because it is a competitive inhibitor of ubiquinol and binds at the quinol oxidation (Q_o) site of the cytochrome bc_1 complex. The uncoupling agent, *p*-triflouromethoxy carbonilcyanide phenylhydrazone (FCCP), was applied in 20 μM concentration to abolish the linkage between the respiratory chain and the phosphorylation system by dissipating the proton-motive force across the membrane.

Induction and relaxation of BChl fluorescence: The induction and relaxation kinetics of the BChl *a* fluorescence of intact cells were measured by a home-built fluorometer (Kocsis *et al.* 2010). The light source for both excitation and monitoring was a laser diode (wavelength of 808 nm and maximum light power of 2 W) that produced rectangular shape of illumination of variable duration and intensity and matched the 800-nm absorption band of the LH2 peripheral antenna of the cells. The BChl fluorescence (centered at 900 nm) was detected in the direction perpendicular to the actinic light beam with a near-infrared-sensitive, large-area (diameter 10 mm), and high-gain Si-avalanche photodiode (APD; model *394-70-72-581*; *Advanced Photonix, Inc.*, USA) protected from the scattered light of the laser by an 850-nm high-pass filter (*RG-850*). Solutions of BChl or *IR-806* dye (*Sigma*) were used as reference for fluorescence yield measurements to correct for any deviations from the rectangular shape and for large-scale fluctuation of the laser diode excitation. The reference signal was adjusted to the same intensity as that of the fluorescence to avoid the possible artifact coming from the nonlinearity of the response of the detector at high light intensity.

Results

Fluorescence induction under high light excitation: Fluorescence induction from the dark state, F_0, to the maximum F_{max} within a couple of μs (Fig. 2) occurred because of the high light intensity (2 W cm^{-2}) and wavelength (808 nm), which matches the absorption band of the peripheral light-harvesting antenna of *R. sphaeroides*. After an additional small rise, it reached F_{max} approximately 1 ms after onset of the excitation. From that level, the fluorescence drops slowly and continuously in several phases to approximately half of the maximal value. A small increase can be seen at the very end of the excitation in the vicinity of the min time range. The kinetic trace is reproducible and reflects reversible changes in the bacterium. This is in contrast to the behavior of free BChl in solution, and the carotenoid-less mutant R-26, where the bleaching of the pigments can be seen in the ms time range under similar induction conditions. It is evident from these experiments that the carotenoids protect the BChl and the photosynthetic apparatus effectively from the oxidative stress caused by the high light intensity. Upon termination of the light excitation, an increase and subsequent decrease of the fluorescence level can be observed at onset of the excitation after dark periods of different durations (data not shown). These are clear signs of relaxation of triplets in the dark and building up in the light. Although the triplets obviously determine the fluorescence kinetics, the contribution of other effects cannot be disclosed in the longer time scale. The definite increase of the fluorescence due to addition of myxothiazol (blocker of the cyt bc_1 complex) and a slight change upon addition of FCCP (uncoupler of electron and proton transfers) demonstrated the effects of cyclic electron transfer and transmembrane pH gradient on the BChl fluorescence, respectively.

Fluorescence induction upon intermittent excitation: The intensity of the excitation can be decreased by intermittent pulsing of the emission of the laser diode. The bacteria were illuminated by a series of light flashes of 3-μs duration and the attenuation of the light intensity was controlled by changing the duty cycle (Fig. 3). The steady-state levels of the fluorescence decreased continuously with a decrease in the duty cycle and showed distinct fast and slow kinetic phases (Fig. 3*A*). At higher duty cycles, single turnover of the RC occurred causing fast decay of the fluorescence level from F_{max}. This is probably due to fast reduction of P^+ by cyt c_2^{2+} bound or closely attached to the RC of *R. sphaeroides*. The slow component reflects the competition of the photochemical charge separation with the stationary flow of the electrons from and in the RC (multiple turnover of the RC). The observation of
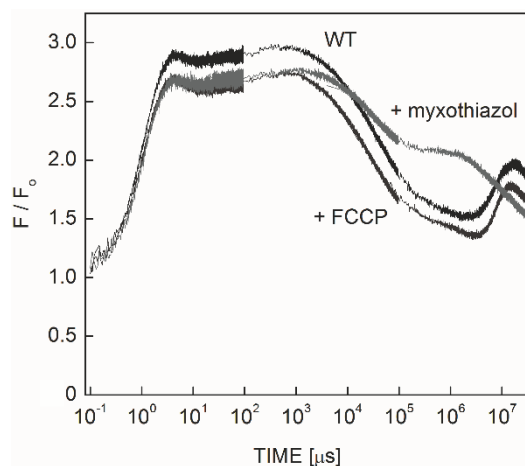

Fig. 2. Fluorescence induction (F/F_0) of anaerobic intact and inhibitor (FCCP and myxothiazol)-treated cells of *Rhodobacter sphaeroides* upon strong and rectangular shape of excitation (intensity 2 W cm^{-2} at 808 nm). F_0 denotes the initial level of fluorescence. Note the logarithmic scales. Each trace was constructed by joining data sets from measurements of three separate time-ranges; these are visible as noise changes in the data.
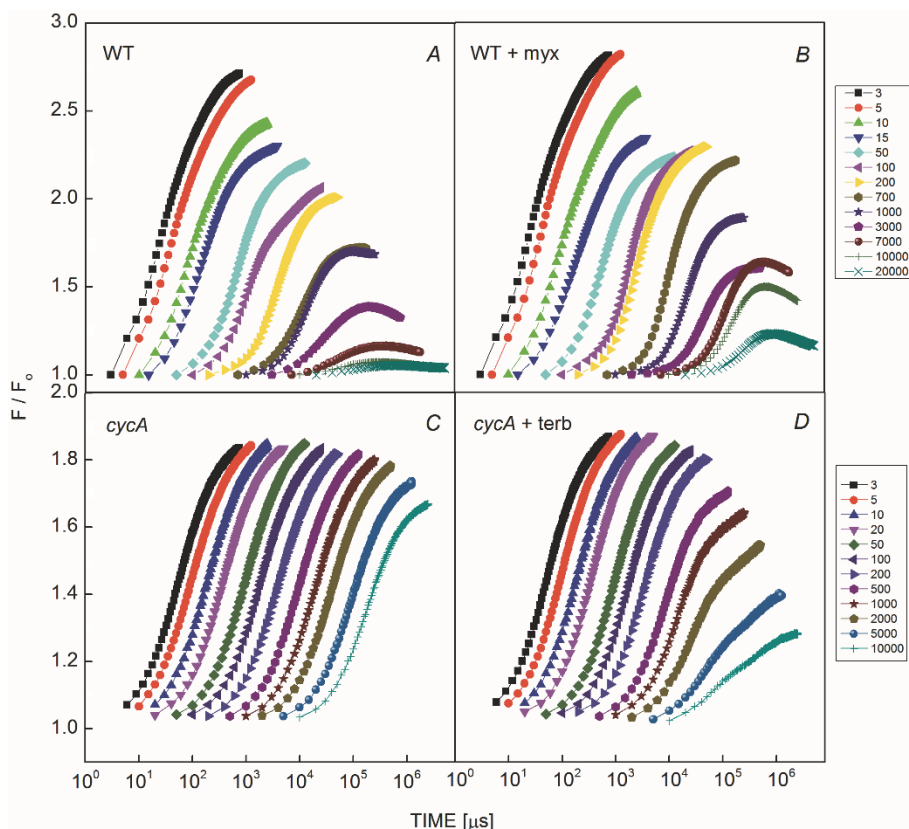
127

Fig. 3. Set of fluorescence induction curves of wild type (*A* und *B*) and cytochrome-less (*C* and *D*) cells of *Rhodobacter sphaeroides* without (*A* and *C*) and with addition of 20 μM myxothiazol (*B*) or 120 μM terbutryne (*D*). The fluorescence was evoked by 250 flashes of 3-μs duration with different dark periods between the neighboring flashes. By changing the duty cycle of the flash series (the ratio of pulse width to pulse period), the fluorescence induction at different light excitations can be measured (see the reciprocals of the duty cycle attached to the color codes). The photochemical rate constant k_I at arbitrary light intensity is determined from the measured value at the highest duty cycle multiplied by the duty cycle of the flash series.

slow decrease of the fluorescence level in the ms time range may reveal essential characteristics of the electron transfer around the RC. Inhibition of electron transfer to the auxiliary oxidants by the cyt bc_1 inhibitor myxothiazol can partly block the slow component without any effects on the initial charge export at the donor and shifts the decay of the fluorescence to larger time scale of seconds (Fig. 3*B*). If the export of the positive charge on the donor side is inhibited, no decrease of the fluorescence is expected anymore. Indeed, flat F_{max} level and only a small subsequent drop in the 10-s time range characterize the mutant in which the *cycA* gene is deleted (Fig. 3*C*). A somewhat faster decrease of the fluorescence level can be observed in the time scale of seconds if the electron transfer was inhibited by addition of terbutryne to the *cycA* mutant (Fig. 3*D*). As the terbutryne closes the acceptor side of the RC by replacing Q_B, both light-induced charges are trapped in the RC. They are removed either by slow reactions with auxiliary oxidants and reductants of unknown origin or by intraprotein charge recombination between P^+ and Q_A^-. The relatively fast kinetics indicates

that the charge recombination should play determining role in re-opening the RC.
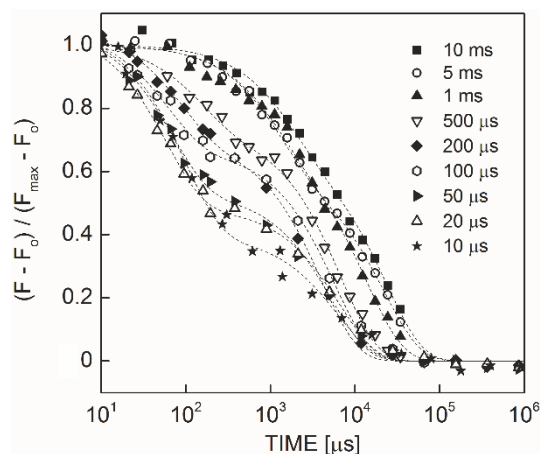

Fig. 4. Relaxation of normalized variable fluorescence generated by intensive light excitation of different durations from 10 μs to 10 ms in whole cells of *Rhodobacter sphaeroides*.

We noted a greater decrease in the magnitude of the variable fluorescence in wild type than that in the *cycA* mutant (compare Figs. 3*A*,*C*). We speculate that this decrease is an indication of minor loss of the connectivity of the light-harvesting pigments to the RC that might include detachment of some BChls from the antenna.

Similarly, complex kinetics can be observed in the relaxation of the fluorescence if the excitation was terminated and the decay of the fluorescence state was tested by weak measuring flashes. Although the relaxation kinetics is inherently multiphasic, the deceleration of the decay after increasing excitation flash duration from 10 μs can be well recognized (Fig. 4). The demonstrative changes in the decay kinetics are terminated after sufficiently long (>1 ms) excitation.

The kinetics derived from induction and relaxation of the fluorescence are highly correlated in the 10^{-5}–10^{-2} s time range (compare Figs. 3, 4). The major changes in the kinetics observed in both cases indicate a common origin of the phenomena.

Discussion

Phases of fluorescence induction under high light excitation: The kinetics of fluorescence induction excited by high intensity laser light is a multiphasic function of time caused by fluorescence quenchers of different origins (Fig. 2). Their kinetic overlap (appearance and disappearance) and strength determine the shape of the observed fluorescence induction. The following phases can be distinguished in dark-adapted intact cells of *R. sphaeroides* under 2 W cm^{-2} laser excitation at 808 nm.

The fluorescence rises to about 90% of the maximum level within several μs. As the rise time increases with the light intensity in linear fashion, this fast initial rise of the fluorescence is the photochemical rise and corresponds to the disappearance of the photochemical quencher PQ_A *via* $PQ_A \rightarrow P^+Q_A^-$.

The single turnover of the RC can produce different redox forms of the RC depending on the rates of re-reduction of P^+ to P *via* bound (or unbound) cyt c_2^{2+} and re-oxidation of Q_A^- *via* interquinone electron transfer to Q_B. If both reactions are carried out, a second turnover can take place which closes the RC completely in form of $P^+(Q_AQ_B)^{2-}$. If this happens, the fluorescence is reaching its maximum. This can occur within 100–200 μs (practically the exchange time of cyt c_2) and leads to an additional rise of the fluorescence to its maximum (100%). The lack of this component is evident in *cycA* mutant where the multiple turnover of the RC is inhibited.

Due to the high light intensity, the carotenoid triplet is formed in parallel with the photochemical quencher. The carotenoid triplet quencher overlaps the photochemical quencher resulting in a decrease of the maximum level of fluorescence, with an occasionally decreasing kinetic phase as observed in nitrogen atmosphere, where the triplet lifetime increases, and a disappearance of the slow phase of the photochemical rise.

As the oxygen-dependent lifetime of the carotenoid triplet is about 5 μs under anaerobic conditions, fast equilibrium is established between the two quenchers that is not perturbed in the μs time range. Later, however, continuous but slow (note the logarithmic scale in Fig. 2) decrease of the fluorescence can be observed in a very broad time scale without any noticeable and characteristic kinetic components. This is in contrast with the earlier findings where six phases in the fluorescence transition kinetics of *R. sphaeroides* were reported with a series of lifetimes from 4 ms to 10 s (Bína *et al.* 2010). The reason for this contradiction is unclear but could be related to the different light conditions and physiological status of the bacteria or to the sudden and unexpected changes in the fluorescence transient. The decline of the fluorescence transient from the maximum to the stationary level is altered very little by the addition of uncoupler FCCP; this indicates that the membrane potential and pH difference makes an insignificant contribution to the changes we observed in the fluorescence induction. Additionally, the membrane potential is more likely to increase than decrease the yield of fluorescence (Bína *et al.* 2010). Based on our results above, we argue that the slow decline of BChl fluorescence after the maximum can be attributed to direct loss of BChl* and/or to a slight increase of triplet concentration. This type of slow modulation can be achieved by molecular oxygen in the bacterial culture. The oxygen-induced deactivation of BChl fluorescence is diffusion controlled and proceeds *via* $S_1 \rightarrow S_0$ internal conversion and $S_1 \rightarrow T_1$ intersystem crossing both causing the decline of BChl fluorescence.

Determination of the rate of cyclic electron flow in intact cells: At low light intensities, a definite drop of the maximum fluorescence level can be observed in accordance with the increase of the half rise time of the fluorescence induction. This is a clear indication of the light intensity limitation of the cyclic electron transport. In this case, the rates of the cyclic electron transfer (overall rate constant k_e) and charge losses in the RC (rate constant k_{loss}, Fig. 1) can compete with that of the light-induced charge separation (rate constant k_I). The observed fluorescence level F is the sum of F_0 and F_{max} weighted by the fractions of open [PQ] and closed [P^+Q^-] RCs, respectively:

$$F = F_0[PQ] + F_{max}\left[P^+Q^-\right] \qquad (1)$$

The kinetics of the RC states is governed by

$$\frac{d[PQ]}{dt} = -k_I[PQ] + \left(k_{loss} + k_e\right)\left[P^+Q^-\right], \qquad (2)$$

where

$$1 = [PQ] + [P^+Q^-] \qquad (3)$$

Introducing the normalized variable fluorescence $F_v = (F - F_0)/(F_{max} - F_0)$, we can get

$$F_v = \left(1 - \frac{k_e + k_{loss}}{k_I + k_e + k_{loss}}\right)\left(1 - e^{-(k_I + k_e + k_{loss}) \cdot t}\right) \qquad (4)$$

Both the amplitude and the rise of the fluorescence induction curves include the rate constants. When the light intensity is high ($k_I \gg k_e + k_{loss}$), the RC can turn over only once in the time range of less than 1 ms and the photochemical quenching determines solely the kinetics of the fluorescence rise to the maximum, F_{max}. If we extend a time range somewhat over 1 ms (by using smaller light intensity), a detectable drop in the fluorescence can be observed. Due to the single turnover of the RC, this phase represents the export of the single positive charge from P^+ (Q_B^- is highly stable on the acceptor side of the RC). This is actually the "loss" term in Eq. 4. If, however, the RC can perform multiple turnovers in the smaller time scale (at lower light intensity), k_{loss} will be neglected and will be part of the overall rate constant of the cyclic electron transport k_e. This is manifested by the gradual decrease of the stationary level (amplitude) of the fluorescence.

The two phases of the drop of the fluorescence can be analyzed based on the amplitudes of Eq. 4: the reciprocal value of F_v should be a linear function of the reciprocal of k_I. The slopes of the straight lines in double reciprocal representation give the rate constants of the thermal reactions k_{loss} and k_e (Fig. 5*A*). The larger rate corresponds to the detachment of cyt c_2^{3+} from the RC (single turnover) and the smaller value to the overall cyclic rate of the electron (multiple turnover).

Another way of determination of the thermal rate constants is the fit of the set of the measured fluorescence induction curves to the exponential functions with variable amplitudes and rate constants given in Eq. 4. Using this procedure, both the steady-state fluorescence levels (amplitudes) and the rates of the fluorescence rise ($k_I + k_e + k_{loss}$) as principal information of Eq. 4 can be utilized. The solution of the problem is highly constrained as there are only two parameters to be fitted to the series of fluorescence transients at different light intensities. Using a least square method, the fit gives reasonable result that can be validated by comparison of Figs. 3*A*, 5*B*.
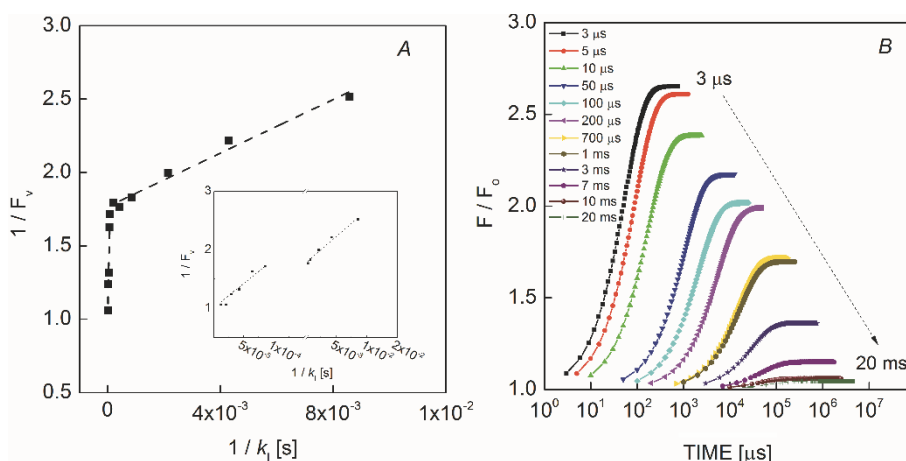

Fig. 5. Evaluation of the fluorescence induction curves of *Rhodobacter sphaeroides* at different excitation light intensities (Fig. 3*A*) according to the simplified electron transfer model in Fig. 1. (*A*) The reaction rate constants of the thermal reactions k_{loss} (single turnover of the RC) and k_e (multiple turnover) can be derived as the slopes of the straight lines in a double reciprocal representation of F_v and k_I (*see* the amplitude of Eq. 4). The inserted panel with divided $1/k_e$ scale exposes both components. (*B*) Global fit of Eq. 4 to the set of fluorescence transients with parameters $k_{loss} = 120 \ \mu s^{-1}$ and $k_e = 11 \ ms^{-1}$ and values of duty cycle given in the box.

It is worthwhile to compare our kinetic data for whole cells with those in chromatophores obtained from other sophisticated flash assays and model calculations. The quinone reduction cycle in chromatophores was estimated to be about 1.6 ms, including 1.2 ms required for the slow binding/release steps (Comayras *et al.* 2005). The half-time required for the released quinol to arrive and bind at the oxidizing site of the cyt bc_1 complex (Q_0) was taken as 5–10 ms (Crofts *et al.* 1983). The overall cycling time of electrons in chromatophore was estimated to be 13 ms (Geyer and Helms 2006) and 22 ms (Bína *et al.* 2010). However, these values are highly influenced by several factors including the arrangement of the electron transfer carriers, the redox conditions of the pools and complexes, and the ways of diffusion of the mobile species. As with the mobile cyt c_2 carriers on the donor side, the quinones in the supercomplex structure are also exposed to confinement (Comayras *et al.* 2005), which shortens the average distance of diffusion between the Q_B and Q_0 sites of the RC and cyt bc_1 complex, respectively (Joliot *et al.* 2005). However, it was found that the rate of diffusion was not the rate limiting step of the electron transfer (Geyer and Helms 2006). By theoretical treatment of the overall operation of the electron transfer, a model was provided

where the significance of the reverse electron flow from the ubiquinone pool (Fig. 1) was also stressed (Klamt *et al.* 2008).

The fluorescence induction and relaxation kinetics offered here 120 μs^{-1} rate constant for the electron exchange between P^+ and cyt c_2^{2+} as the major pathway of charge export on the donor side of the intact cell of *R. sphaeroides*. This process offers the dominating component in single turnover of the RC. In multiple turnover, however, when the cyclic (from RC to RC) electron transport is operating, a rate constant of 11 ms^{-1} was found which falls in the wide range of values discussed above. The cyclic electron transfer includes several steps and the slowest one determines the overall measured rate. The bottle neck can be the binding/ unbinding of mobile quinone and cytochrome c_2 species to the RC (and to the cyt bc_1 complex) and/or their pathway through the corresponding pools. The effects of the redox state of the pools, intactness of the macromolecular complexes, and the crowding of the molecular constituents of the apparatus can have major influence on the observed kinetics as was demonstrated under different treatments of the cells. As these parameters are determined by the physiological status of the bacteria, the fluorescence kinetic traces can be used to monitor the internal electron transfer processes and the photosynthetic capacity if the proper protocol and evaluation method are available. The present work served this purpose together with congratulations to Govindjee for his birthday. We wish him many happy returns of the day.

References

Asztalos E., Italiano F., Milano F. *et al*.: Early detection of mercury contamination by fluorescence induction of photosynthetic bacteria. – Photoch. Photobio. Sci. **9**: 1218-1223, 2010.

Asztalos E., Sipka G., Maróti P.: Fluorescence relaxation in intact cells of photosynthetic bacteria: donor and acceptor side limitations of reopening of the reaction center. – Photosynth. Res. **124**: 31-44, 2015.

Bína D., Litvín R., Vácha F.: Absorbance changes accompanying the fast fluorescence induction in the purple bacterium *Rhodobacter sphaeroides*. – Photosynth. Res. **105**: 115-121, 2010.

Chi S.C., Mothersole D.J., Dilbeck P. *et al*.: Assembly of functional photosystem complexes in *Rhodobacter sphaeroides* incorporating carotenoids from the spirilloxanthin pathway. – Biochim. Biophys. Acta **1847**: 189-201, 2015.

Comayras F., Jungas C., Lavergne J.: Functional consequences of the organization of the photosynthetic apparatus in *Rhodobacter sphaeroides*. I. Quinone domains and excitation transfer in chromatophores and reaction center antenna complexes. – J. Biol. Chem. **280**: 11203-11213, 2005.

Crofts A.R., Meinhardt S.W., Jones K.R., Snozzi M.: The role of the quinone pool in the cyclic electron-transfer chain of *Rhodopseudomonas sphaeroides*: A modified Q-cycle mechanism. – Biochim. Biophys. Acta **723**: 202-218, 1983.

de Rivoyre M., Ginet N., Bouyer P., Lavergne J.: Excitation transfer connectivity in different purple bacteria: a theoretical and experimental study. – Biochim. Biophys. Acta **1797**: 1780-1794, 2010.

Donohue T.J., Kaplan S.: Genetic techniques in rhodospirillaceae. – Methods Enzymol. **204**: 459-485, 1991.

Duysens L.N.M.: Transfer of light energy within the pigment systems present in photosynthesizing cells. – Nature **168**: 548-550, 1951.

Geyer T., Helms V.: A spatial model of the chromatophore vesicles of *Rhodobacter sphaeroides* and the position of the cytochrome bc_1 complex. – Biophys. J. **91**: 921-926, 2006.

Joliot P., Joliot A., Vermeglio A.: Fast oxidation of the primary electron acceptor under anaerobic conditions requires the organization of the photosynthetic chain of *Rhodobacter sphaeroides* in supercomplexes. – BBA-Bioenergetics **1706**: 204-214, 2005.

Kautsky H., Hirsch A.: [New experiments on carbonic acid assimilation.] – Naturwissenschaften **19**: 964, 1931. [In German]

Kis M., Asztalos E., Sipka G., Maróti P.: Assembly of photosynthetic apparatus in *Rhodobacter sphaeroides* as revealed by functional assessments at different growth phases and in synchronized and greening cells. – Photosynth. Res. **122**: 261-273, 2014.

Kis M., Sipka G., Asztalos E. *et al*.: Purple non-sulfur photosynthetic bacteria monitor environmental stresses. – J. Photoch. Photobio. B **151**: 110-117, 2015.

Klamt S., Grammel H., Straube R. *et al*: Modelling the electron transport chain of purple nonsulfur bacteria. – Mol. Syst. Biol. **4**: 156, 2008.

Koblizek M., Shih J.D., Breitbart S.I. *et al*.: Sequential assembly of photosynthetic units in *Rhodobacter sphaeroides* as revealed by fast repetition rate analysis of variable bacteriochlorophyll a fluorescence. – Biochim. Biophys. Acta **1706**: 220-231, 2005.

Kocsis P., Asztalos E., Gingl Z., Maróti P.: Kinetic bacteriochlorophyll fluorometer. – Photosynth. Res. **105**: 73-82, 2010.

Maróti P.: Kinetics and yields of bacteriochlorophyll fluorescence: redox and conformation changes in reaction center of *Rhodobacter sphaeroides*. – Eur. Biophys. J. **37**: 1175-1184, 2008.

Maróti P.: Induction and relaxation of bacteriochlorophyll fluorescence in photosynthetic bacteria. – In: Pessarakli M. (ed): Handbook of Photosynthesis, 3rd ed. Pp. 463-483. CRC Press, Boca Raton – London – New York 2016.

Niederman R.A.: Development and dynamics of the photosynthetic apparatus in purple phototrophic bacteria. – Biochim. Biophys. Acta **1857**: 232-246, 2016.

Sambrook J., Fritsch E.F., Maniatis T.: Molecular cloning: a laboratory manual, 2nd ed. Page A.1. Cold Spring Harbor Laboratory Press, New York 1989.

Sisтröm W.R.: The kinetics of the synthesis of photopigments in *Rhodopseudomonas spheroides*. – J. Gen. Microbiol. **28**: 607-616, 1962.

Sisтröm, W.R., Transfer of chromosomal genes mediated by plasmid r68.45 in *Rhodopseudomonas sphaeroides*. – J. Bacteriol. **131**: 526-532, 1977

Stirbet A., Govindjee: Chlorophyll a fluorescence induction: a personal perspective of the thermal phase, the J-I-P rise. – Photosynth. Res. **113**: 15-61, 2012.

Trissl H.W.: Antenna organization in purple bacteria investigated by means of fluorescence induction curves. – Photosynth. Res. **47**: 175-185, 1996.